Supporting Information

Synthesis, polymorphism, and shape complementarity-induced co-crystallization of hexanuclear Co(II) clusters capped by a flexible heteroligand shell

Michał Terlecki[a], Arkadiusz Kornowicz,[b] Kornel Sacharczuk,[a] Iwona Justyniak,[b] and Janusz Lewiński*[a,b]*

[a]Faculty of Chemistry, Warsaw University of Technology, Noakowsiego 3, 00-664 Warsaw, Poland

[b]Institute of Physical Chemistry, Polish Academy of Sciences, Kasprzaka 44/52, 01-224 Warsaw, Poland

Table of contents

Cobalt(II) acetate purification

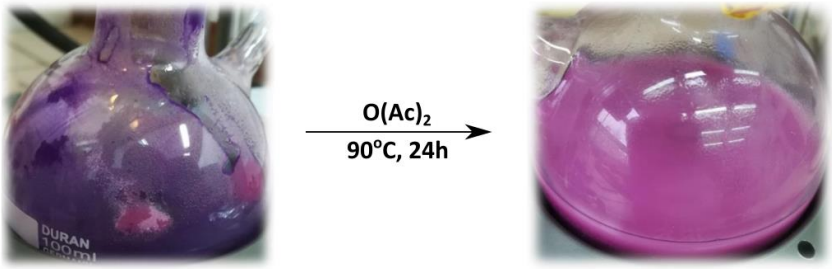

Figure S1. Color change during purification of commercial cobalt(II) acetate.

TGA Analysis

According to the literature thermal decomposition of $Co(OAc)_2 \cdot 4H_2O$ is a complicated multi-step process.[1] The mass decrease to 150°C is associated with dehydration and partial elimination of acetic acid with the formation of Co-OH species. Then above 260°C there is further elimination of acetic acid leading to deprotonation of OH groups. Finally, at about 350°C decomposition of organic parts occurs leading to cobalt oxides. A similar multi-step decomposition is observed in commercial and thermally treated $Co(OAc)_2$ (Figure S2 and S3), with a mass decrease below 150°C of about 10% and 3%, respectively. These values quite well reflect the water content in estimated (based on elemental analysis) formulas for both reagents: $[Co(OH)_{0.34}(OAc)_{1.66}] \cdot 0.70H_2O$ (calc. water cont. 7.2%) and $[Co(OH)_{0.28}(OAc)_{1.72}] \cdot 0.12H_2O$ (calc. water cont. 1.3%), respectively (note, that experimental mass decrease is grater likely due to partial elimination of acetic acid). In turn, the TGA curve for purified $Co(OAc)_2$ shows only a three-step decomposition above 240°C (Figure S3), indicating the absence of water or OH groups in the structure.

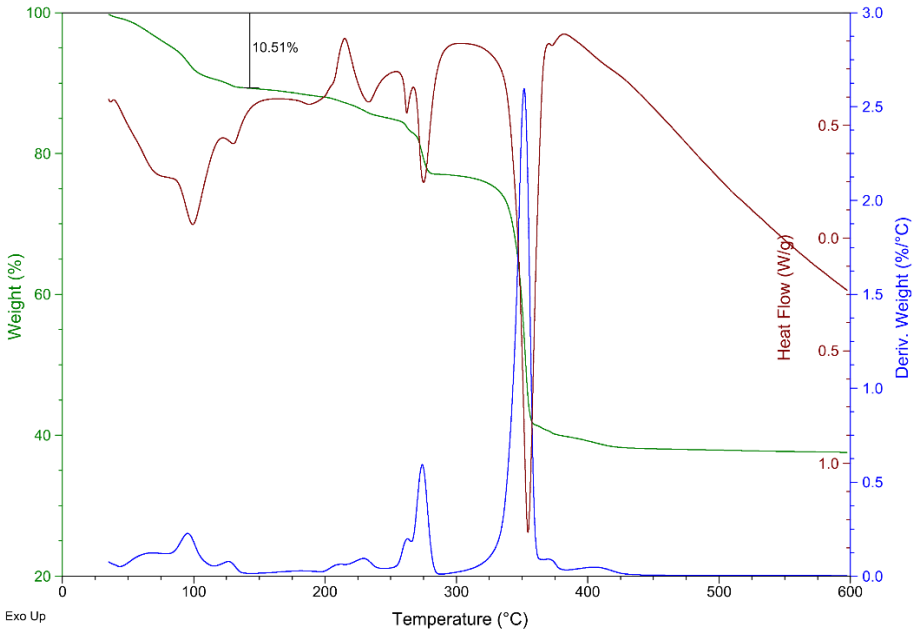

Figure S2. TGA-DSC plot for commercial cobalt(II) acetate.

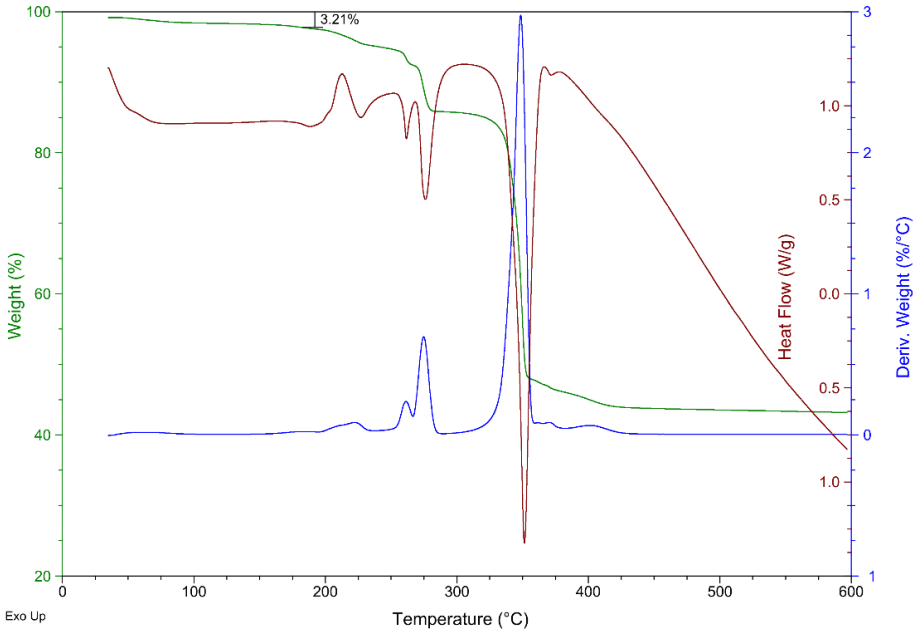

Figure S3. TGA-DSC plot for thermally treated cobalt(II) acetate.

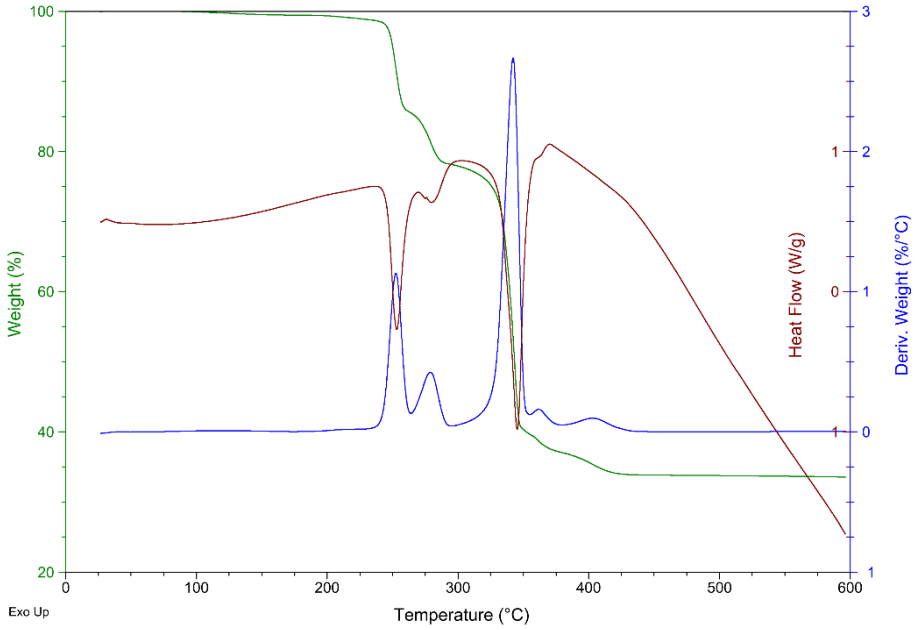

Figure S4. TGA-DSC plot for purified cobalt(II) acetate.

PXRD Analysis

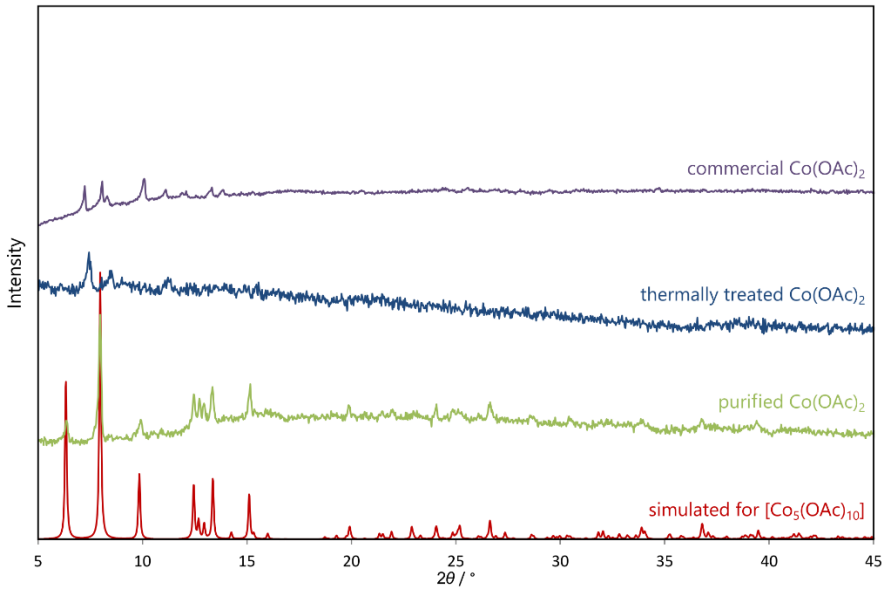

Figure S5. PXRD patterns simulated for $[Co_5(OAc)_{10}]$[2] and measured for commercial, thermally treated, and purified $Co(OAc)_2$ reagents.

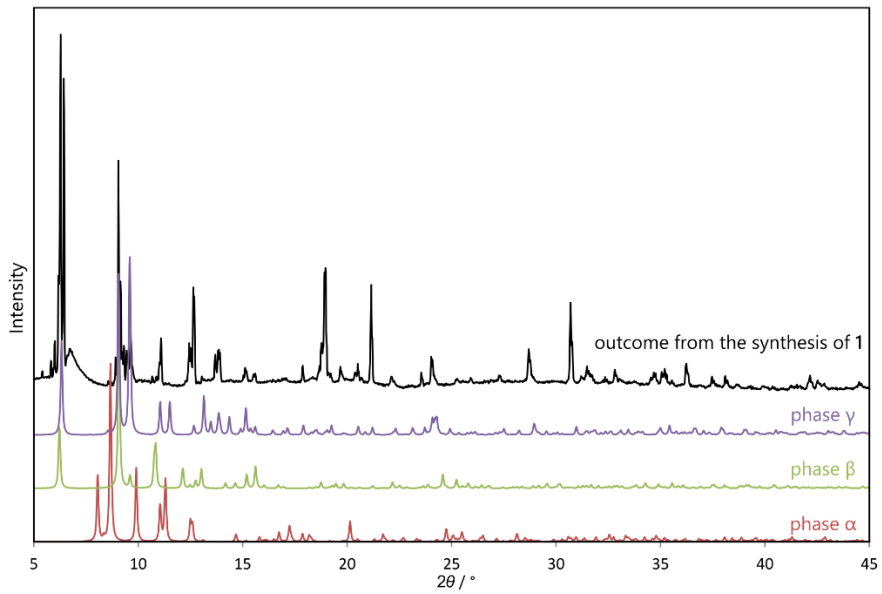

Figure S6. PXRD patterns simulated for phases α, β, and γ of complex **1** and measured for the outcome from the synthesis of **1**.

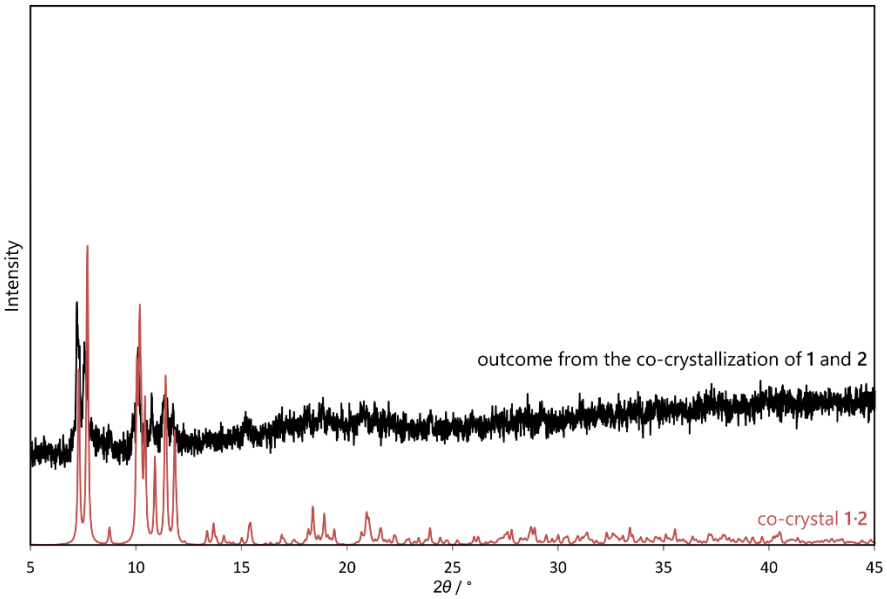

Figure S7. PXRD patterns simulated for co-crystal **1·2** and measured for for the outcome from the co-crystallization of **1** and **2**.

X-Ray crystallographic data

Table S1. Crystal data and structure refinement for **1(α)**

Empirical formula	$C_{44}H_{86}Co_6N_6O_{16}$	
Formula weight	1308.76	
Temperature	100(2) K	
Wavelength	0.71073 Å	
Crystal system	Monoclinic	
Space group	P 21/n	
Unit cell dimensions	a = 11.4060(4) Å	a= 90°.
	b = 11.6220(4) Å	b= 104.348(2)°.
	c = 21.8380(8) Å	g = 90°.
Volume	2804.56(17) $Å^3$	
Z	2	
Density (calculated)	1.550 Mg/m^3	
Absorption coefficient	1.801 mm^{-1}	
F(000)	1364	
Theta range for data collection	2.553 to 27.353 °.	
Index ranges	-14<=h<=14, -15<=k<=14, -26<=l<=28	
Reflections collected	10537	
Independent reflections	5775 [R(int) = 0.0387]	
Completeness to theta = 25.000°	93.9 %	
Refinement method	Full-matrix least-squares on F^2	
Data / restraints / parameters	5775 / 0 / 327	
Goodness-of-fit on F^2	1.104	
Final R indices [I>2sigma(I)]	R1 = 0.0367, wR2 = 0.0794	
R indices (all data)	R1 = 0.0434, wR2 = 0.0823	
Largest diff. peak and hole	0.402 and -0.493 $e.Å^{-3}$	

[a] $R1 = \Sigma||Fo| - |Fc||/\Sigma|Fo|$. [b] $wR2 = [\Sigma w(Fo^2 - Fc^2)^2/\Sigma w(Fo^2)^2]^{1/2}$

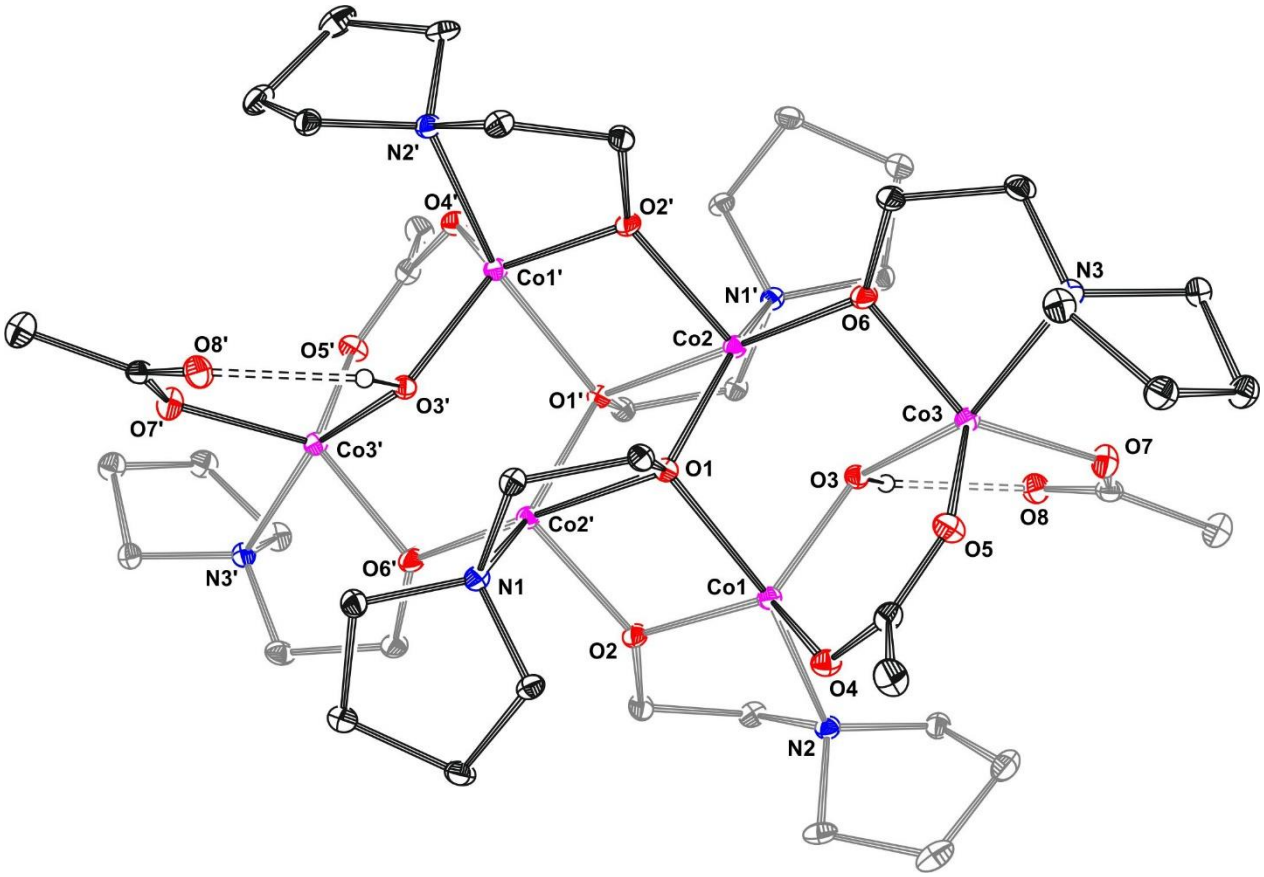

Figure. S8. Molecular structure of **1(α)** with thermal ellipsoids set at 30% probability. Hydrogen atoms have been omitted for clarity. Symmetry transformations used to generate equivalent atoms: (*-x+1, -y+1, -z+1*).

Table S2. Crystal data and structure refinement for **1(β)**

Empirical formula	$C_{44}H_{86}Co_6N_6O_{16}$	
Formula weight	1308.76	
Temperature	100(2) K	
Wavelength	0.71073 Å	
Crystal system	Monoclinic	
Space group	P 21/c	
Unit cell dimensions	a = 14.2057(4) Å	a= 90°.
	b = 12.0883(4) Å	b= 93.260(3)°.
	c = 16.4530(7) Å	g = 90°.
Volume	2820.78(17) $Å^3$	
Z	2	
Density (calculated)	1.541 Mg/m^3	
Absorption coefficient	1.791 mm^{-1}	
F(000)	1364	
Theta range for data collection	2.872 to 26.995°.	
Index ranges	-18<=h<=17, -13<=k<=15, -21<=l<=20	
Reflections collected	13583	
Independent reflections	6056 [R(int) = 0.0543]	
Completeness to theta = 25.242°	99.8 %	
Refinement method	Full-matrix least-squares on F^2	
Data / restraints / parameters	6056 / 0 / 327	
Goodness-of-fit on F^2	1.109	
Final R indices [I>2sigma(I)]	R1 = 0.0425, wR2 = 0.1003	
R indices (all data)	R1 = 0.0585, wR2 = 0.1130	
Largest diff. peak and hole	0.693 and -0.584 $e.Å^{-3}$	

[a] $R1 = \Sigma||Fo| - |Fc||/\Sigma|Fo|$. [b] $wR2 = [\Sigma w(Fo^2 - Fc^2)^2/\Sigma w(Fo^2)^2]^{1/2}$

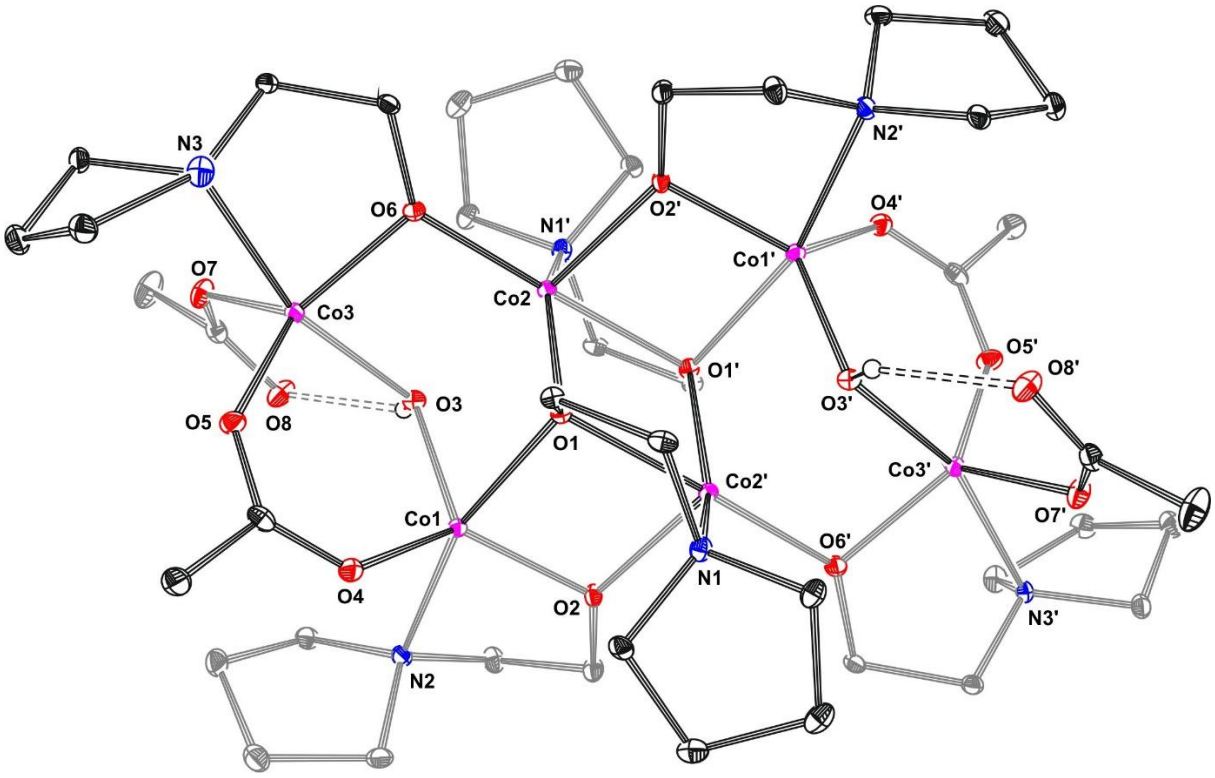

Figure. S9. Molecular structure of **1(β)** with thermal ellipsoids set at 30% probability. Hydrogen atoms have been omitted for clarity. Symmetry transformations used to generate equivalent atoms: (*-x+1, -y+1, -z+1*).

Table S3. Crystal data and structure refinement for **1(γ)**

Empirical formula	$C_{44}H_{86}Co_6N_6O_{16}$	
Formula weight	1308.76	
Temperature	100(2) K	
Wavelength	0.71073 Å	
Crystal system	Orthorhombic	
Space group	P c a 21	
Unit cell dimensions	a = 12.6327(3) Å	a= 90°.
	b = 15.3660(3)Å	b= 90°.
	c = 27.9274(5) Å	g = 90°.
Volume	5421.10(19) $Å^3$	
Z	4	
Density (calculated)	1.604 Mg/m^3	
Absorption coefficient	1.864 mm^{-1}	
F(000)	2728	
Theta range for data collection	3.024 to 26.999 °.	
Index ranges	-15<=h<=9, -19<=k<=14, -34<=l<=35	
Reflections collected	19815	
Independent reflections	10589 [R(int) = 0.0372]	
Completeness to theta = 25.242°	99.8 %	
Absorption correction	Semi-empirical from equivalents	
Refinement method	Full-matrix least-squares on F^2	
Data / restraints / parameters	10589 / 3 / 662	
Goodness-of-fit on F^2	1.045	
Final R indices [I>2sigma(I)]	R1 = 0.0427, wR2 = 0.0862	
R indices (all data)	R1 = 0.0539, wR2 = 0.0940	
Largest diff. peak and hole	1.317 and -0.471 $e.Å^{-3}$	

[a] $R1 = \Sigma||Fo| - |Fc||/\Sigma|Fo|$. [b] $wR2 = [\Sigma w(Fo^2 - Fc^2)^2/\Sigma w(Fo^2)^2]^{1/2}$

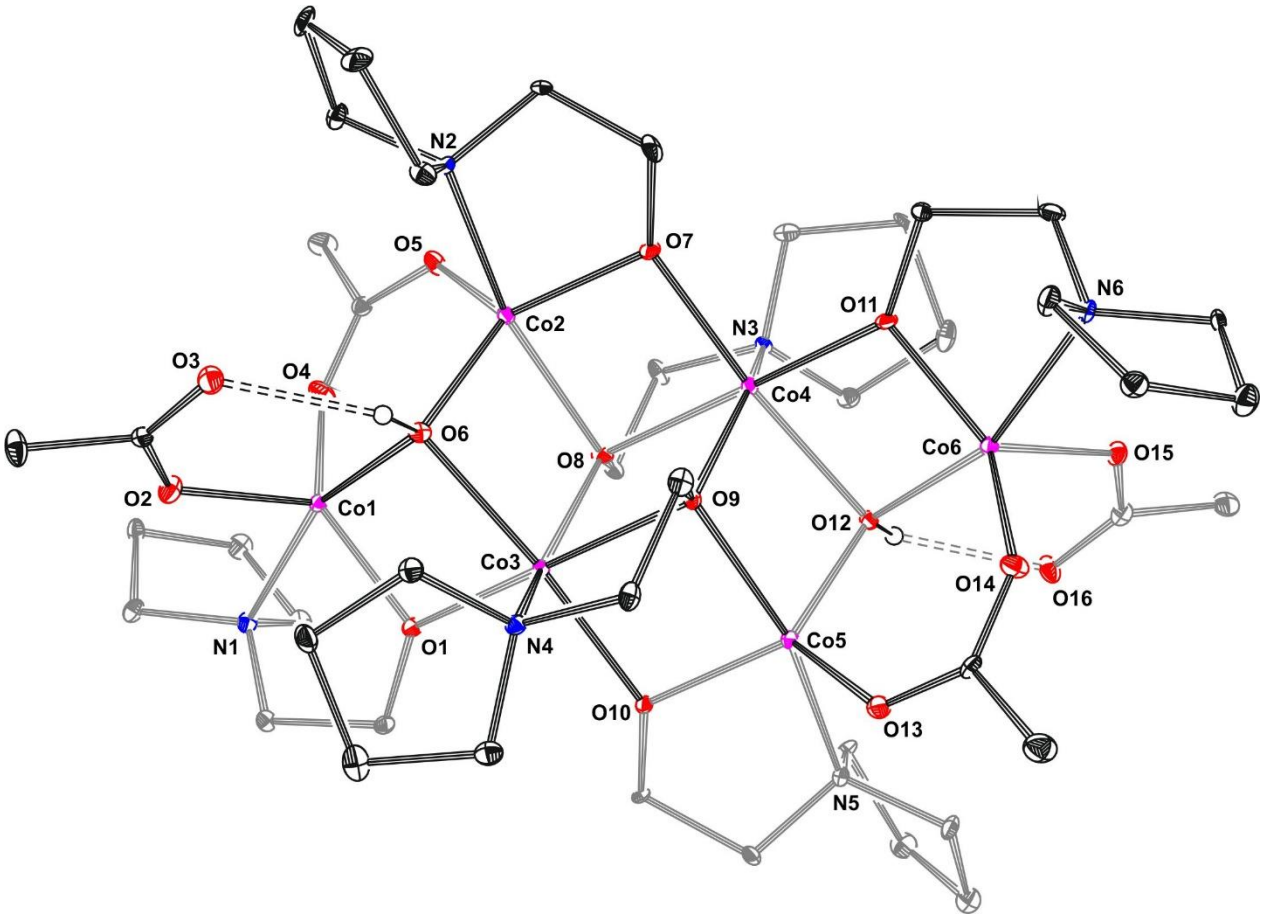

Figure. S10. Molecular structure of **1(γ)** with thermal ellipsoids set at 30% probability. Hydrogen atoms have been omitted for clarity.

Table S4. Crystal data and structure refinement for **2**

Empirical formula	$C_{48}H_{90}Co_6N_6O_{18}$	
Formula weight	1392.83	
Temperature	100(2) K	
Wavelength	0.71073 Å	
Crystal system	Monoclinic	
Space group	P 21/c	
Unit cell dimensions	a = 12.2702(2) Å	a= 90°.
	b = 13.7088(3) Å	b= 91.439(2)°.
	c = 17.3126(3) Å	g = 90°.
Volume	2911.23(9) $Å^3$	
Z	2	
Density (calculated)	1.589 Mg/m^3	
Absorption coefficient	1.743 mm^{-1}	
F(000)	1452	
Theta range for data collection	2.972 to 29.214°.	
Index ranges	-16<=h<=16, -18<=k<=18, -23<=l<=20	
Reflections collected	15030	
Independent reflections	6780 [R(int) = 0.0234]	
Completeness to theta = 25.242°	99.6 %	
Absorption correction	Semi-empirical from equivalents	
Refinement method	Full-matrix least-squares on F^2	
Data / restraints / parameters	6780 / 6 / 365	
Goodness-of-fit on F^2	1.081	
Final R indices [I>2sigma(I)]	R1 = 0.0366, wR2 = 0.0831	
R indices (all data)	R1 = 0.0436, wR2 = 0.0861	
Largest diff. peak and hole	0.792 and -0.436 $e.Å^{-3}$	

[a] $R1 = \Sigma||Fo| - |Fc||/\Sigma|Fo|$. [b] $wR2 = [\Sigma w(Fo^2 - Fc^2)^2/\Sigma w(Fo^2)^2]^{1/2}$

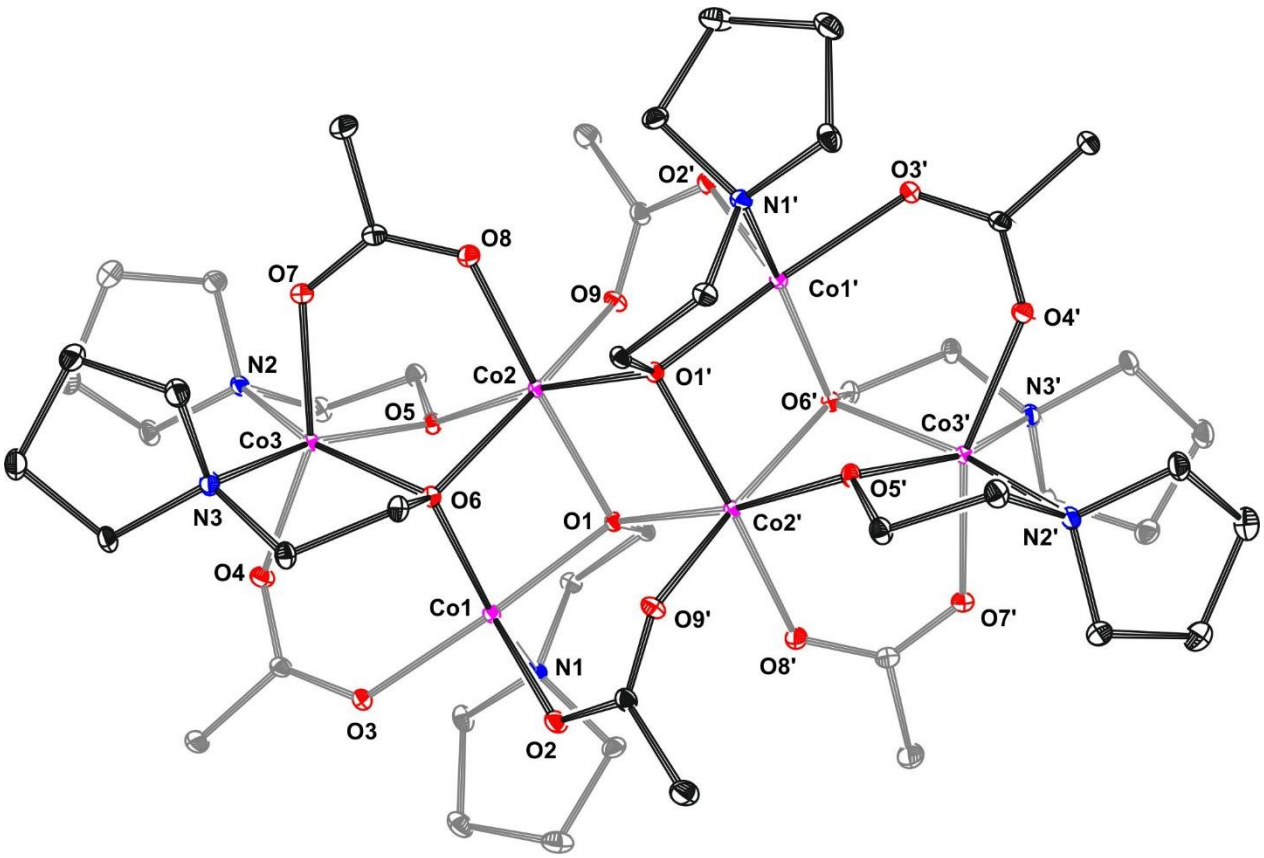

Figure. S11. Molecular structure of **2** with thermal ellipsoids set at 30% probability. Hydrogen atoms have been omitted for clarity. Symmetry transformations used to generate equivalent atoms: (*-x, -y, -z*).

Table S5. Crystal data and structure refinement for **1-2**

Empirical formula	$C_{92}H_{176}Co_{12}N_{12}O_{34}$	
Formula weight	2701.60	
Temperature	100(2) K	
Wavelength	0.71073 Å	
Crystal system	Triclinic	
Space group	P -1	
Unit cell dimensions	a = 10.1181(4) Å	a= 93.061(3)°.
	b = 16.2501(6) Å	b= 91.191(3)°.
	c = 17.1906(7) Å	g = 91.462(3)°.
Volume	2820.83(19) $Å^3$	
Z	1	
Density (calculated)	1.590 Mg/m^3	
Absorption coefficient	1.795 mm^{-1}	
F(000)	1408	
Theta range for data collection	3.079 to 27.000°.	
Index ranges	-12<=h<=12, -20<=k<=18, -21<=l<=21	
Reflections collected	22897	
Independent reflections	12114 [R(int) = 0.0280]	
Completeness to theta = 25.242°	99.8 %	
Absorption correction	Semi-empirical from equivalents	
Refinement method	Full-matrix least-squares on F^2	
Data / restraints / parameters	12114 / 42 / 710	
Goodness-of-fit on F^2	1.040	
Final R indices [I>2sigma(I)]	R1 = 0.0321, wR2 = 0.0682	
R indices (all data)	R1 = 0.0406, wR2 = 0.0736	
Largest diff. peak and hole	0.536 and -0.559 $e.Å^{-3}$	

[a] $R1 = \Sigma||Fo| - |Fc||/\Sigma|Fo|$. [b] $wR2 = [\Sigma w(Fo^2 - Fc^2)^2/\Sigma w(Fo^2)^2]^{1/2}$

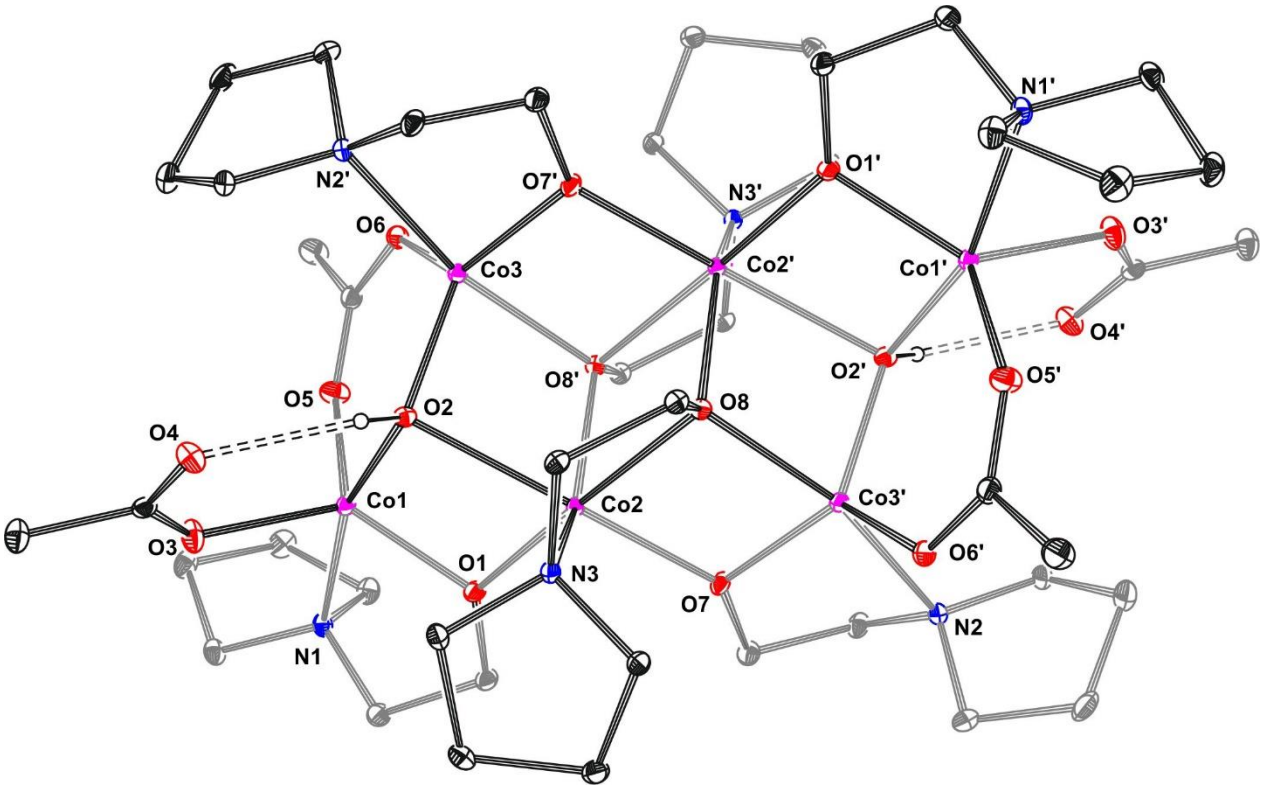

Figure. S12. Molecular structure of **1-2** with thermal ellipsoids set at 30% probability. Hydrogen atoms have been omitted for clarity. Symmetry transformations used to generate equivalent atoms: (*-x, -y+2, -z*), (*-x+1, -y+1, -z+1*).

Coordination geometry analysis

Analysis of the coordination sphere geometry of Co(II) centers in the presented structures was conducted employing the continuous shape measurement (CShM)[3] (lower the CShM values indicate better fit to given geometry) using SHAPE softwere.[4] The results are presented in Table S6 and S7.

Table S6. CShM parameters for five-coordinated Co(II) centers in crystal structures of **1**, **2** and **1·2**

	CShM							
	1(α)		**1(β)**		**1(γ)**			
Geometry	Co1	Co3	Co1	Co3	Co1	Co2	Co5	Co6
Vacant octahedron (C_{4v})	6.194	3.614	6.560	5.752	5.235	3.807	3.930	4.762
Trigonal bipyramid (D_{3h})	**1.737**	**2.460**	**1.759**	**1.283**	**2.042**	**2.420**	**2.334**	**1.965**
Spherical square pyramid (C_{4v})	4.160	**2.006**	4.560	4.259	4.024	**2.260**	**2.269**	3.628
Johnson trigonal bipyramid J_{12} (D_{3h})	2.871	3.909	2.864	2.842	3.297	3.431	3.387	3.146

Table S6 c.d.

	CShM			
	2	**1** in **1·2**		**2** in **1·2**
Geometry	Co1	Co1	Co3	Co6
Vacant octahedron (C_{4v})	**1.574**	5.503	6.315	**1.487**
Trigonal bipyramid (D_{3h})	3.455	**1.635**	**1.833**	3.546
Spherical square pyramid (C_{4v})	**1.138**	3.734	4.240	**0.966**
Johnson trigonal bipyramid J_{12} (D_{3h})	6.189	3.152	2.960	6.192

Table S7. CShM parameters for six-coordinated Co(II) centers in crystal structures of **1**, **2** and **1·2**

	CShM								
	1(α)	**1(β)**	**1(γ)**		**2**		**1** in **1·2**	**2** in **1·2**	
Geometry	Co2	Co2	Co3	Co4	Co2	Co3	Co2	Co4	Co5
Pentagonal pyramid (C_{5v})	18.624	18.473	19.186	19.064	25.188	16.933	17.205	16.850	24.446
Octahedron (O_h)	**3.272**	**3.202**	**3.025**	**3.057**	**1.076**	**4.937**	**3.933**	**4.672**	**1.058**
Trigonal prism (D_{3h})	9.898	9.732	8.927	8.958	12.959	7.646	9.471	8.114	13.864
Johnson pentagonal pyramid J_2 (C_{5v})	22.899	22.759	23.612	23.579	28.861	20.297	21.251	20.161	28.131

Hirshfeld Surface analysis:

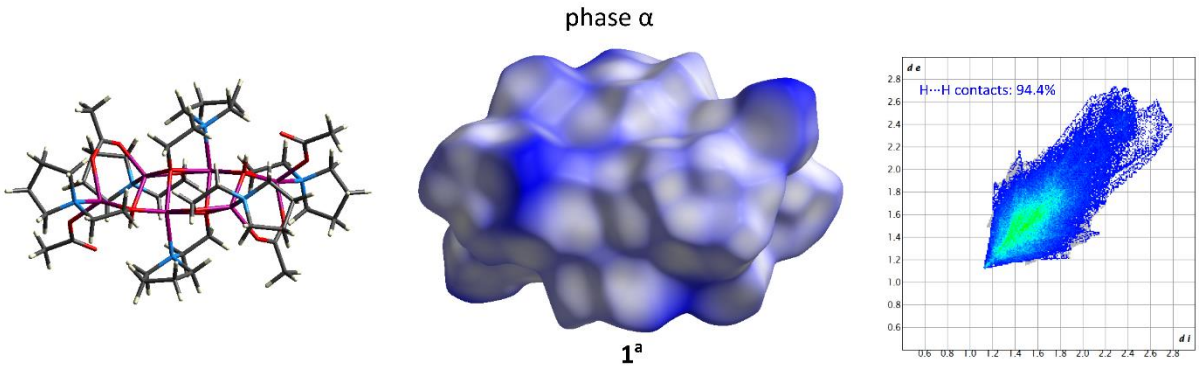

Figure S13. Hirshfeld surface (mapped with d_{norm}) and fingerprint plot of cluster **1**[a] in phase α.

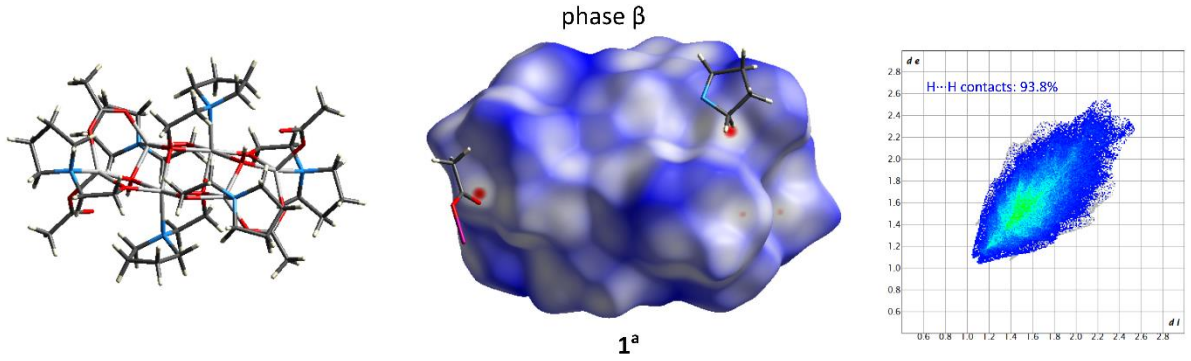

Figure S14. Hirshfeld surface (mapped with d_{norm}) and fingerprint plot of cluster **1**[a] in phaseβ.

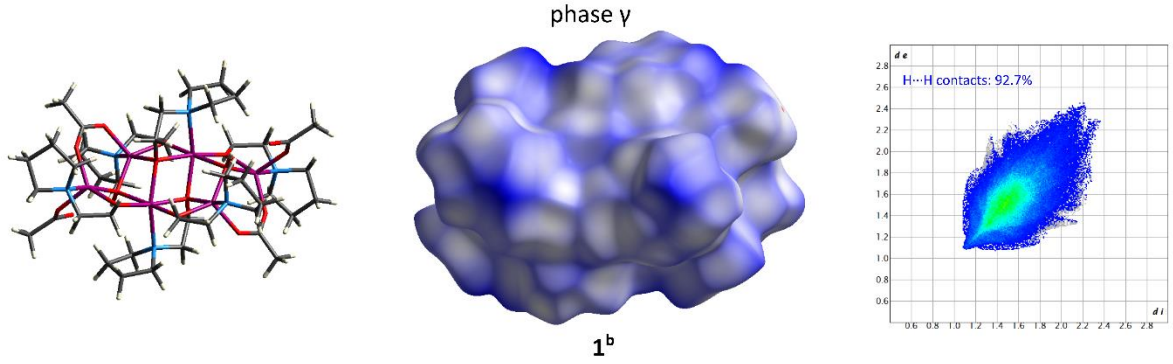

Figure S15. Hirshfeld surface (mapped with d_{norm}) and fingerprint plot of cluster **1**[b] in phase γ.

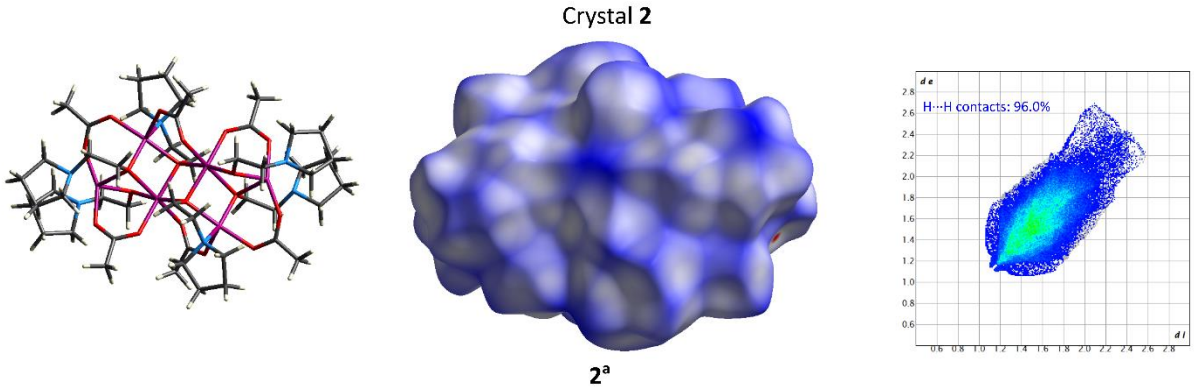

Figure S16. Hirshfeld surface (mapped with d_{norm}) and fingerprint plot of cluster **2ª**.

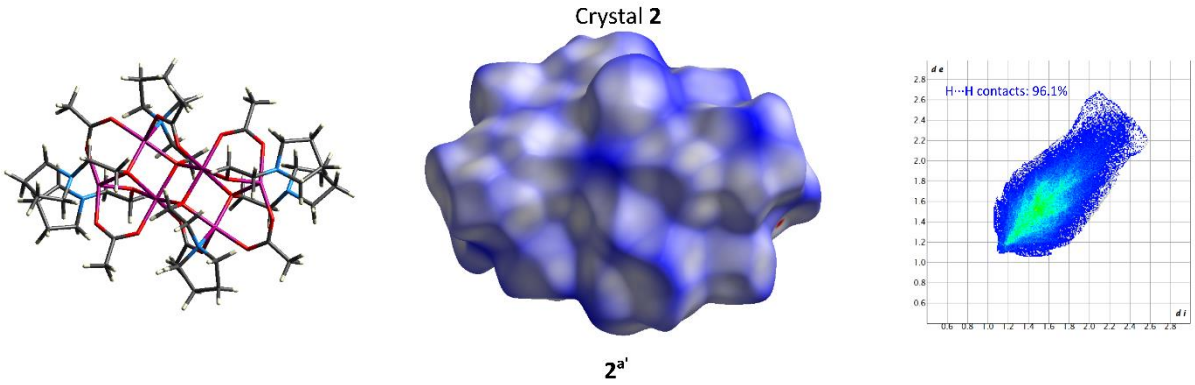

Figure S17. Hirshfeld surface (mapped with d_{norm}) and fingerprint plot of cluster **2ª'**.

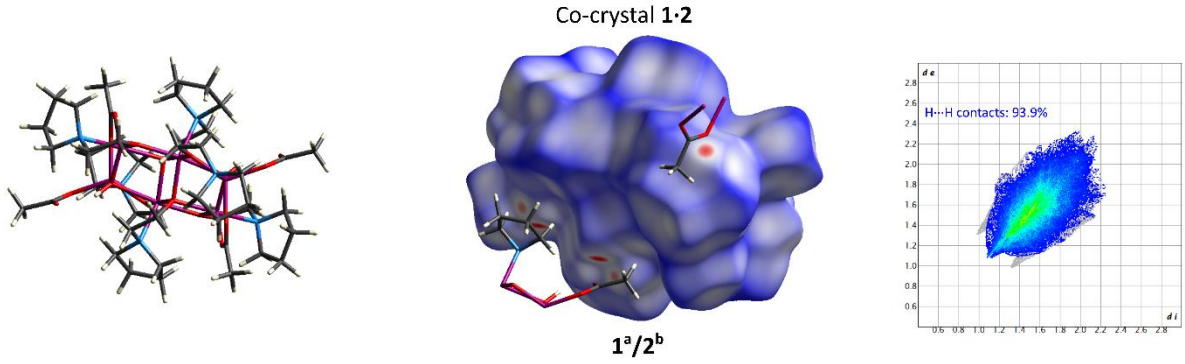

Figure S18. Hirshfeld surface (mapped with d_{norm}) and fingerprint plot of cluster **1ª** in co-crystal **1·2** (including co-former **2ᵇ**).

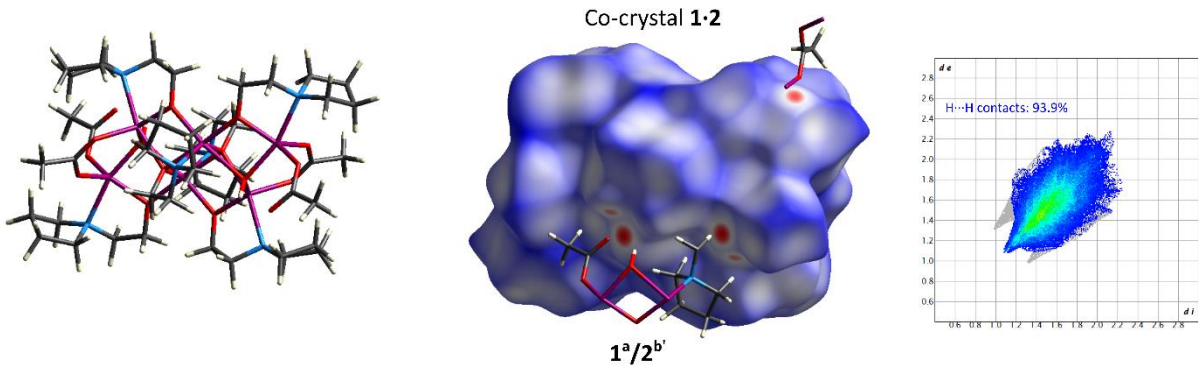

Figure S19. Hirshfeld surface (mapped with d_{norm}) and fingerprint plot of cluster **1ª** in co-crystal **1·2** (including co-former **2ᵇ'**).

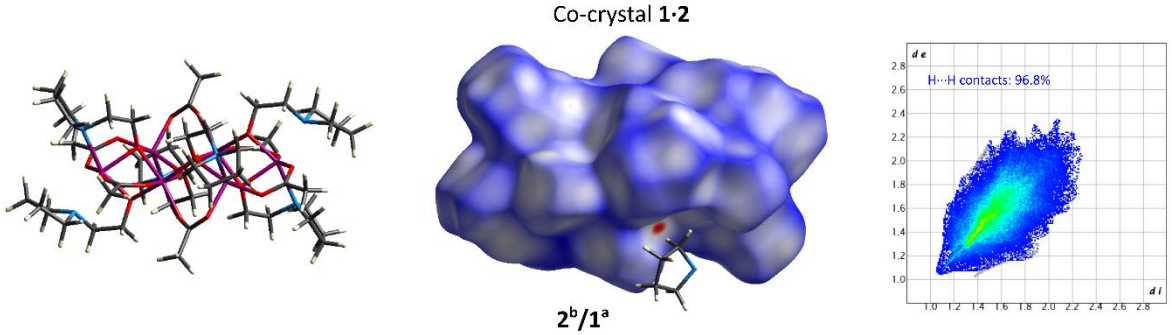

Figure S20. Hirshfeld surface (mapped with d_{norm}) and fingerprint plot of cluster **2ᵇ** in co-crystal **1·2**.

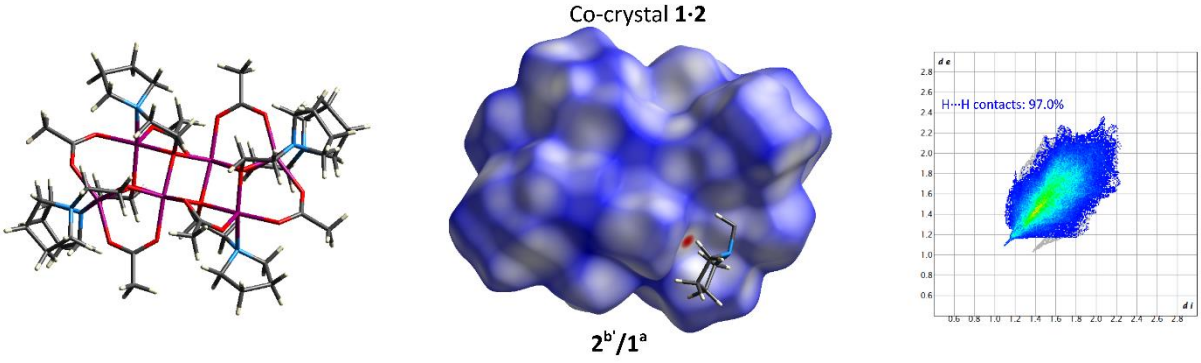

Figure S21. Hirshfeld surface (mapped with d_{norm}) and fingerprint plot of cluster **2ᵇ'** in co-crystal **1·2**.

Table S8. Selected Hirshfeld surface (HS) parameters for monocomponent crystals of **1** and **2** and co-crystal **1·2**.

Molecule	HS area [Å²]	H···H contacts area [%]	H···O contacts area [%]	d_i [Å]			d_e [Å]		
				min	mean	max	min	mean	max
1[a] in phase α	808.13	94.4	4.5	1.126	1.616	2.803	1.127	1.632	2.749
1[a] in phase β	796.83	93.8	5.5	1.048	1.614	2.555	1.046	1.630	2.563
1[b] in phase γ	818.98	92.7	6.3	1.080	1.560	2.373	1.079	1.575	2.479
2[a] in **2**	819.24	96.0	3.6	1.062	1.581	2.593	1.061	1.594	2.703
2[a'] in **2**	824.43	96.1	3.5	1.061	1.576	2.583	1.061	1.590	2.701
1[a](with **2**[b]) in **1·2**	800.24	93.9	5.6	0.995	1.565	2.293	0.995	1.579	2.349
1[a](with **2**[b']) in **1·2**	797.46	93.9	5.5	0.995	1.561	2.293	0.995	1.574	2.316
2[b] in **1·2**	844.35	96.8	3.0	1.055	1.586	2.298	1.036	1.604	2.367
2[b'] in **1·2**	845.17	97.0	2.7	1.096	1.579	2.271	1.035	1.596	2.367

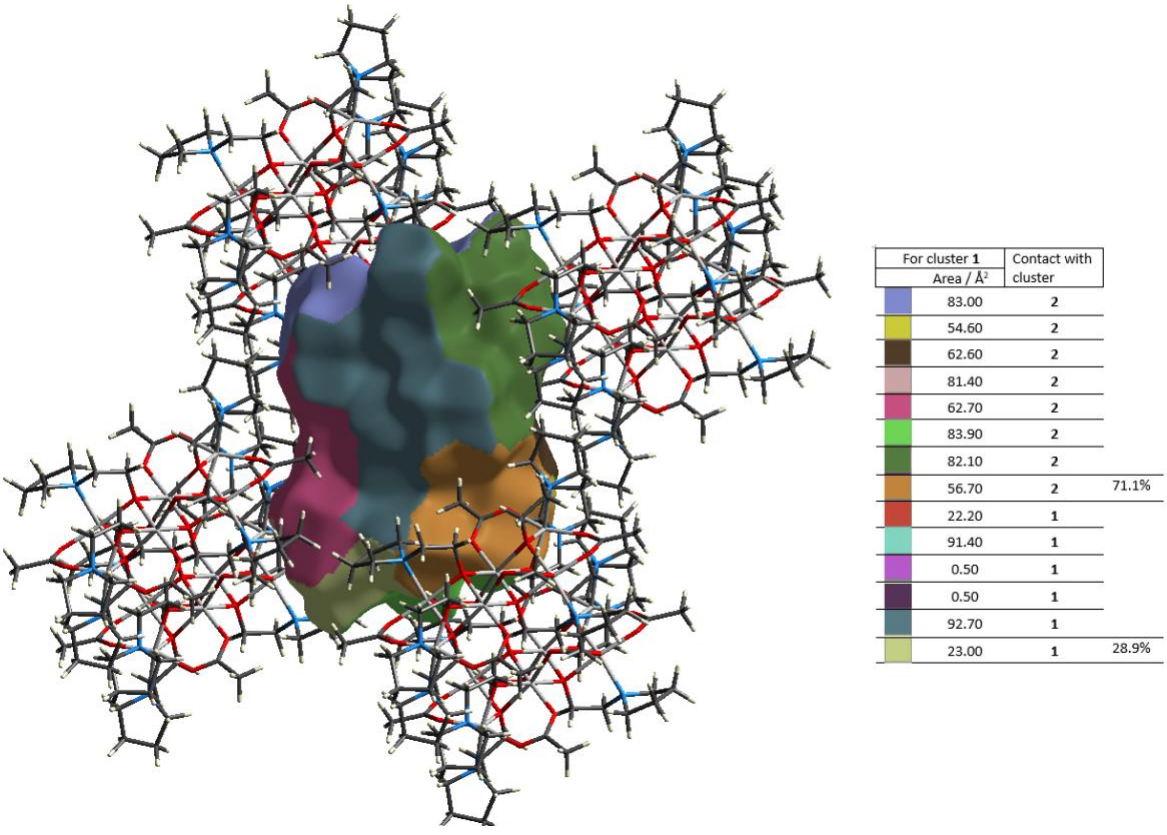

Figure S22. Analysis of HS contacts of cluster **1** in co-crystal **1·2**.

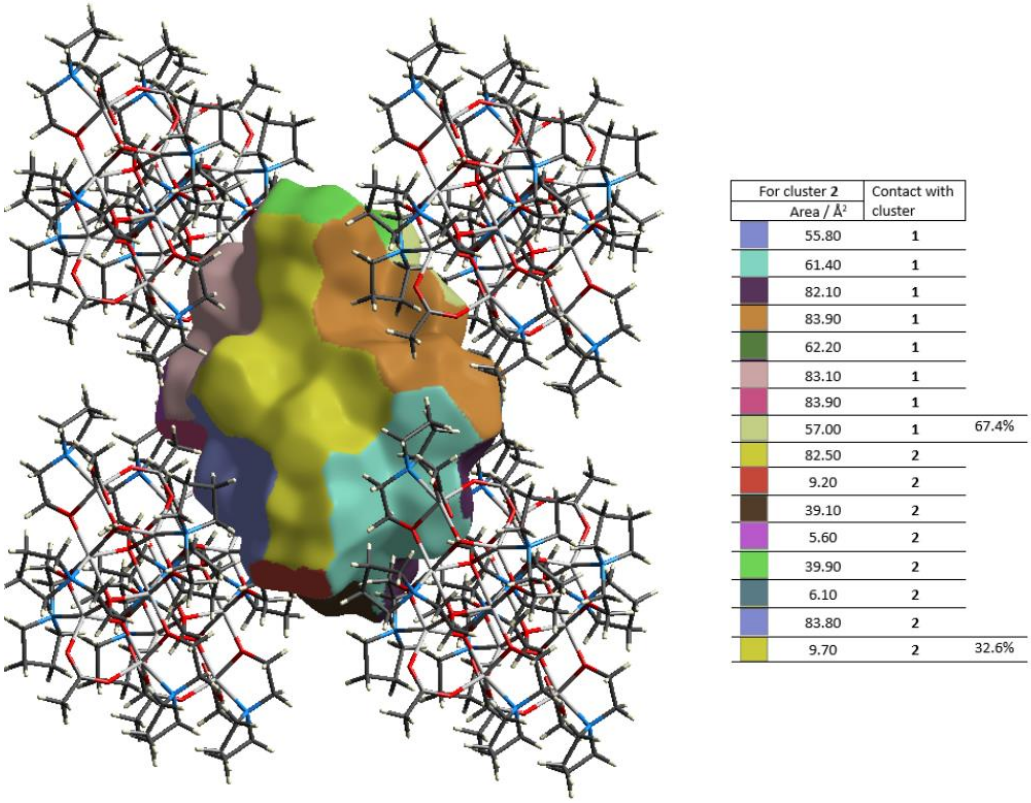

For cluster 2 Area / Å²	Contact with cluster	
55.80	1	
61.40	1	
82.10	1	
83.90	1	
62.20	1	
83.10	1	
83.90	1	
57.00	1	67.4%
82.50	2	
9.20	2	
39.10	2	
5.60	2	
39.90	2	
6.10	2	
83.80	2	
9.70	2	32.6%

Figure S23. Analysis of HS contacts of cluster **1** in co-crystal **1·2**.

References:

1 R. Kuhlman, G. L. Schimek and J. W. Kolis, *Inorg. Chem.*, 1999, **38**, 194–196.

2 G. Zhang, J. Lin, D. Guo, S. Yao and Y. Tian, *Zeitschrift für Anorg. und Allg. Chemie*, 2010, **636**, 1401–1404.

3 H. Zabrodsky, S. Peleg and D. Avnir, *J. Am. Chem. Soc.*, 1992, **114**, 7843–7851.

4 M. Llunell, D. Casanova, J. Cirera, P. Alemany and S. Alvarez, 2013, Version 2.1.